



Entrainment, diapycnal mixing and transport in three-dimensional bottom gravity current simulations using the Mellor–Yamada turbulence scheme

Tal Ezer *

Program in Atmospheric and Oceanic Sciences, Princeton University, Princeton, NJ 08544-0710, USA

Received 30 March 2004

Available online 25 June 2004

Abstract

The diapycnal mixing, entrainment and bottom boundary layer (BBL) dynamics in simulations of dense overflows are evaluated, using a generalized coordinate ocean model that can utilize terrain-following or z -level vertical grids and uses the Mellor–Yamada (M–Y) turbulence closure scheme to provide vertical mixing coefficients. Results from idealized dense water overflow experiments at resolutions of 10 and 2.5 km using a terrain-following vertical coordinates compare very well with the results from a nonhydrostatic ocean model (MITgcm) with resolution of 0.5 km, and also with the basic observed properties of the Denmark Straits overflow. At both 10 and 2.5 km resolutions the dilution of the bottom plume is comparable to the nonhydrostatic results, indicating that the M–Y scheme represents the subgrid-scale mixing very well. The 2.5 and 0.5 km model simulations are surprisingly very similar even in the details of the eddy field structure. Strong diapycnal mixing and large entrainment result in more than doubling the plume transport within ~ 100 km from the source, similar to observations, while further downstream small detrainment and reduced transport occur. However, when the diapycnal mixing associated with the mixing scheme is eliminated by setting $K_H = 0$, the terrain-following model results closely resemble the results of isopycnal models whereas the dense plume slides farther downslope while its transport continue to increase indefinitely. On the other hand, when eliminating the bottom Ekman transport associated with the mixing scheme by setting $K_M = 0$, the model results resemble the results of a stepped-topography z -level model without BBL. The bottom Ekman transport associated with the M–Y vertical mixing was found to be responsible for $\sim 20\%$ of the downslope transport of the bottom plume. The vertical mixing coefficient shows a spatially variable asymmetric structure across the bottom plume indicating a stronger mixing over

* Tel.: +1-609-258-1318; fax: +1-609-258-2850.

E-mail address: ezer@splash.princeton.edu (T. Ezer).

a thicker BBL in the upslope side of the plume, and a weaker mixing over a thinner BBL in the downslope side of the plume.

© 2004 Elsevier Ltd. All rights reserved.

Keywords: Numerical modeling; Overflow; Ocean mixing

1. Introduction

Recent observations (Girton and Sanford, 2003) and laboratory experiments (Cenedese et al., 2004) of dense overflow gravity currents and their interaction with sloping bottoms indicate complex flow dynamics that may involve eddies, bottom mixing and entrainment. For example the mixing characteristics and spreading of the Denmark Strait overflow show highly variable currents with strong entrainment and transport changes within ~ 100 – 200 km from the sill (Girton and Sanford, 2003). It is a great challenge for ocean models, in particular for coarse resolution climate models, to accurately simulate such flows, whereas overflow simulations largely depend on the model configuration and the subgrid-scale mixing parameterization (Griffies et al., 2000).

The representation of topography in coarse resolution climate models may also be a challenge. The difficulty in simulating overflow processes using z -level grids with stepped topography has been indicated in numerous studies (Gerdes, 1993; Beckmann and Döscher, 1997; Winton et al., 1998; Pacanowski and Gnanadesikan, 1998; Griffies et al., 2000; Ezer and Mellor, 2004). Therefore, various ways of either improving the bottom representation in models (Adcroft et al., 1997; Pacanowski and Gnanadesikan, 1998) or adding various bottom boundary layer (BBL) schemes (Beckmann and Döscher, 1997; Campin and Gosse, 1999; Killworth and Edwards, 1999; Song and Chao, 2000) have been developed. However, those BBL schemes do not completely solve the problem, and may need numerical improvements or calibration. Overflows representation in terrain-following ocean models (Jiang and Garwood, 1996; Jungclaus and Mellor, 2000; Käse et al., 2003; Jungclaus et al., 2001) and in isopycnal ocean models (Papadakis et al., 2002) may seem easier to achieve since bottom plumes to large extent are driven by their density anomaly relative to the background stratification, and the flow is mostly parallel to the bottom. Nevertheless, finding appropriate parameterizations for diapycnal mixing in hydrostatic models of all types is still an area of ongoing research (Price and Barringer, 1994; Griffies et al., 2000; Hallberg, 2000; Papadakis et al., 2002; Legg et al., in press).

While using very high resolution (<1 km grids) nonhydrostatic ocean models (Marshall et al., 1998; Ozgokmen and Chassignet, 2002; Legg et al., in press) for large scale problems may still be impractical, they can be used for comparison and calibration of mixing parameterizations in coarser resolution models. The dynamics of overflows mixing and entrainment (DOME) initiative established an idealized model setup to investigate the dynamics of bottom plumes and a framework to compare different models. For example, the DOME setup was used to compare terrain-following and z -level models (Ezer and Mellor, 2004), and to compare isopycnal and z -level models as well as hydrostatic and nonhydrostatic models (Legg et al., in press). The same configuration will be used here as well.

Ezer and Mellor (2004) used the generalized coordinate model of Mellor et al. (2002) with the Mellor–Yamada (M–Y) turbulence scheme (Mellor and Yamada, 1982). They show that a

terrain-following model provides reasonable simulations of overflows in basin-scale (100 km grid) and in regional (10 km grid) simulations, but the M–Y mixing was not working well with a stepped-topography z -level grid (10 km horizontal resolution), resulting in excess diapycnal mixing and insufficient downslope penetration of the dense plume. With 2.5 km z -level grid the BBL structure starts converging toward the terrain-following model solution and closer to the structure of observed overflows. Adding shaved cells as in Legg et al. (in press) or any of the other BBL parameterizations may improve the simulations of overflows in the z -level calculations without the need to increase resolution that much, but there are still some numerical problems or calibration issues in those BBL schemes that are not completely resolved.

This study is a follow-up on Ezer and Mellor (2004), using the same model and configuration, but adding experiments, first with higher resolution (2.5 km) terrain-following grid that are compared with the nonhydrostatic calculations of Legg et al. (in press), and second, special cases to isolate the effect of the M–Y turbulence scheme on diapycnal mixing and transport of the bottom plume. Countless studies looked at the M–Y scheme's influence on shallow regions, surface mixed layers and compared it with other mixing schemes (Martin, 1985; Ezer, 2000; Warner et al., in press), but very few studies looked at its influence on the BBLs of the deep ocean. One example is the modeling study of the interaction between bottom plumes and the sloping bottom in the deep (at 4000–5000 m) North Atlantic ocean by Ezer and Weatherly (1990) who found large spatial variations in the mixing coefficient near the bottom due to changes in stratification and shear across the plume. Similar BBL processes may apply to dense overflow plumes, which is the focus of this study.

2. The ocean model and the DOME setup

The Princeton ocean model with generalized coordinate system (POMgcs) is described in detail by Mellor et al. (2002). Unlike the original free surface, three-dimensional, primitive equation POM code (Blumberg and Mellor, 1987), which used a standard vertical sigma coordinates with the same relative layer thickness independent of depth, this version allows almost any combination of terrain-following or z -level distribution of layers that may vary in space and time (i.e., an adaptable grid). The so called s -coordinate system (Song and Haidvogel, 1994) used in the regional ocean modeling system, ROMS, and in other terrain-following models (Haidvogel et al., 2000; Ezer et al., 2002) can be a special case of the generalized coordinates; a standard z -level grid with stepped topography is another possible option.

The idealized model configuration for the DOME setup is described in detail in Ezer and Mellor (2004) and in Legg et al. (in press). The domain includes a basin of 1100×800 km with maximum depth of 3600 m and a 1% steep slope which connects to a 100 km wide and 600 m deep embayment where a dense overflow of 5 Sv (1 Sverdrup = $10^6 \text{ m}^3 \text{ s}^{-1}$) is imposed over background stratification (Fig. 1). The imposed dense inflow is in a geostrophic balance to minimize instability and excess mixing within the embayment. A linear equation of state (with constant salinity) is used so that the maximum density difference ($\rho_{\max} - \rho_{\min}$ in Fig. 1b) between the surface and the deepest layers, and between the surface and the dense bottom layer in the embayment both have $\Delta\sigma_T = 2 \text{ kg m}^{-3}$. All grids use 50 vertical layers except the high resolution z -level grid which used 88 layers (see Ezer and Mellor, 2004, for grids detail). To help analyze the

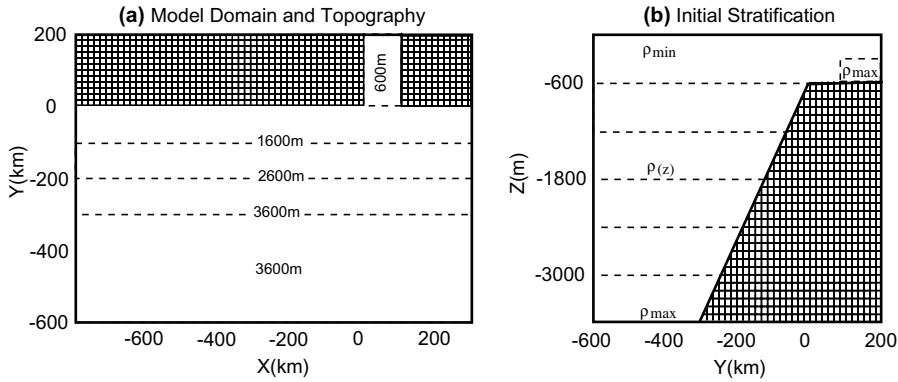


Fig. 1. (a) Top view of the model domain and bottom topography, and (b) side view of a cross-sections at $x = 0$ and the initial stratification.

development of the dense water plume, a tracer, with value $c = 1$, was injected into the dense water in the embayment; initially $c = 0$ everywhere else.

Constant horizontal diffusivity (A_H) and viscosity ($A_M = 5A_H$) are used with values of $A_H = 10 \text{ m}^2 \text{ s}^{-1}$ for the 2.5 km grids and $A_H = 100 \text{ m}^2 \text{ s}^{-1}$ for the 10 km grids (see Ezer and Mellor, 2004, for model sensitivity to diffusivity values in overflow simulations). The vertical mixing coefficients are obtained from the Mellor–Yamada turbulence scheme (Mellor and Yamada, 1982),

$$(K_M, K_H) = \ell q(S_M, S_H), \quad (1)$$

with the turbulence kinetic energy, $q^2/2$ and the turbulence length scale, ℓ , are calculated from two prognostic equations that take into account horizontal and vertical diffusion, shear and buoyancy production and turbulence dissipation. S_M and S_H are stability functions which depend on the Richardson number. A small background vertical diffusivity of $2 \times 10^{-5} \text{ m}^2 \text{ s}^{-1}$ is added to (1), however, in the special experiments where mixing coefficients are null, the background value was also set to zero.

3. Results

3.1. The effect of vertical grid type and horizontal resolution on the bottom plume structure

A comparison between the terrain-following and the z -level coordinates for the DOME experiments using 10 km horizontal grids have been discussed in detail in Ezer and Mellor (2004). In Fig. 2, additional experiments with the two coordinate types using 2.5 km grids are also compared with results of the nonhydrostatic MIT general circulation model (MITgcm) which uses a 0.5 km horizontal grid. Note however, that even at 0.5 km resolution the nonhydrostatic model does not fully resolve shear instability mixing at the interface of the plume and the ambient layers, so it may be called a “mixing permitting”, not a “mixing resolving” model (Legg et al., in press). Several interesting points emerge from this comparison.

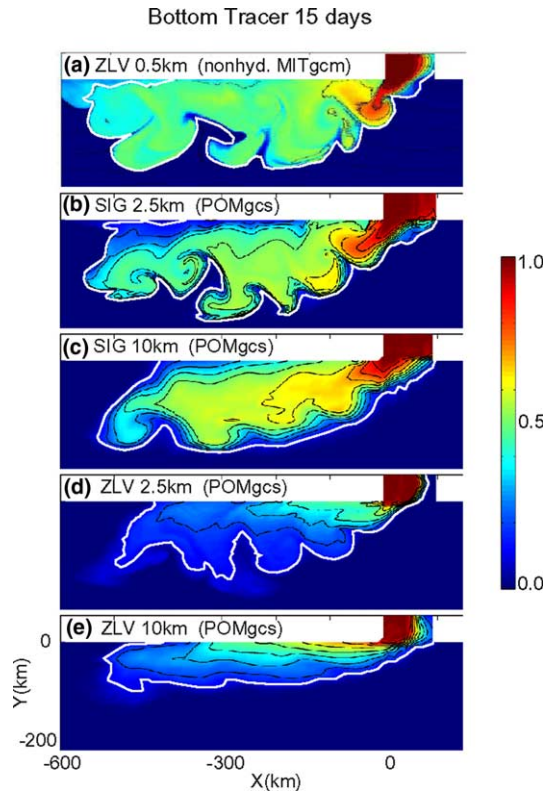


Fig. 2. Tracer concentration at the bottom layer after 15 days simulations with different models: (a) nonhydrostatic MIT general circulation model (MITgcm) with 0.5 km resolution; (b) hydrostatic Princeton Ocean Model with general coordinate system (POMgcs) using a sigma grid with 2.5 km resolution; (c) same as (b) but with 10 km resolution; (d) POMgcs using a stepped z -level grid with 2.5 km resolution; (e) same as (d) but with 10 km resolution. The edge of the plume with tracer value around 0.2 is indicated by the white contour.

1. The z -level model with either 10 or 2.5 km grid (Fig. 2d and e) shows more diapycnal mixing due to the large vertical mixing over the stepped topography (Ezer and Mellor, 2004) than the sigma coordinate model does (Fig. 2b and c). As a result, the plume in the z -level model is too diluted relative to the results of the nonhydrostatic model (Fig. 2a). The plume also tends to remain near the coast in the z -level models but has farther downstream extension in the sigma models. The thickness of the plume is about 250 m in the 10 and 2.5 km sigma model, and in the 2.5 km z -level model, quite close to the observed plume downstream of the Denmark Strait (Girton and Sanford, 2003), however, it is twice as thick, about 450 m in the 10 km z -level model (Ezer and Mellor, 2004). It should be noted though that unlike the stepped z -level topography in POMgcs the MITgcm with 2.5 km z -level grid presented in Legg et al. (in press) has partial bottom cells, thus compared somewhat better with the 0.5 km model which also has partial cells.
2. Using a 2.5 km grid in either the z -level or the sigma models (Fig. 2b and d), produce eddies that are comparable in size to those of the 0.5 km model, indicating that for the

characteristics of this overflow, with a Rossby radius of deformation of $\sim 20\text{--}50$ km, a model resolution of 2.5 km may be sufficient. The importance of meandering and eddies for mixing of overflow plumes has been indicated in previous studies using numerical models, observations and laboratory experiments (Jiang and Garwood, 1996; Jungclaus et al., 2001; Girton and Sanford, 2003; Cenedese et al., 2004). The entrainment rate and the thickness of simulated plumes are influenced by the ability of the model to resolve these eddies (Ezer and Mellor, 2004).

3. Because of the non-linear nature of the plume dynamics and the complicated turbulent mixing involved in the interaction of the plume with the overlaying water and with the sloping bottom, it is somewhat surprising to see that the details of the plume structure and its dilution in the 2.5 km sigma model after 15 days (Fig. 2b) are so similar to those obtained by a completely different model with a horizontal resolution five times finer and nonhydrostatic dynamics (Fig. 2a). In fact, the 2.5 km POMgcs results resemble the 0.5 km MITgcm results even more than the results of the 2.5 km version of the same MITgcm model do (shown in Legg et al., in press). Note for example, the similarity in the “hammer head” like deep-water intrusion near $x = -300$ km. However, some differences remain—for example, the plume separated from the coast in the sigma model but not in the MIT model, a feature also typical to our coarser resolution z -level grid of Fig. 2e. It will be shown later that this difference may relate to the Ekman transport in the BBL.

The above comparisons, and in particular point #3, indicate that the BBL mixing and the entrainment with the overlaying waters are simulated well in the sigma model when vertical (diapycnal) mixing is represented by the M–Y turbulence scheme. In the M–Y model the unresolved subgrid-scale turbulence is solved by prognostic equations for the turbulence velocity and length scale so there is no need for specific parameterizations of entrainment. In other models entrainment may be estimated for example from Richardson or Froude number parameterizations (Price and Barringer, 1994; Hallberg, 2000).

Details of the structure of the plume near the bottom after 40 days (Fig. 3) reveals an asymmetric spatial structure of the mixing coefficient with large values near the north (upslope) side of the plume, where significant mixing extends for over 100 m from the bottom, but with smaller mixing coefficient on the downslope side, where significant mixing is limited to ~ 25 m off the bottom. Similar asymmetry has been found in past simulations of other dense plumes on sloping bottoms (e.g., Ezer and Weatherly, 1990), and possibly in recent observations of the Denmark Straits (Fig. 6 in Girton and Sanford, 2003, indicates larger bottom flow and bottom stress on the upslope side of the plume). The reason for this asymmetry is the Ekman BBL dynamic which causes the velocity to spiral from almost along isobath in the upper plume toward more downslope direction near the bottom (toward the left in Fig. 3). Therefore, the downslope Ekman transport destabilizes the stratification on the upslope side, pushing lighter bottom water of the interior under the dense plume water, the result is a large K_M that creates a well mixed BBL (note the vertical density contours around $x = -25$ km). On the other (downslope) side of the plume, the Ekman transport pushes the dense source water under lighter interior waters, the result is a thin and stable BBL with less vertical mixing. Note also that the downslope edge of the plume reached the depth in which its buoyancy relative to the interior is almost neutral.

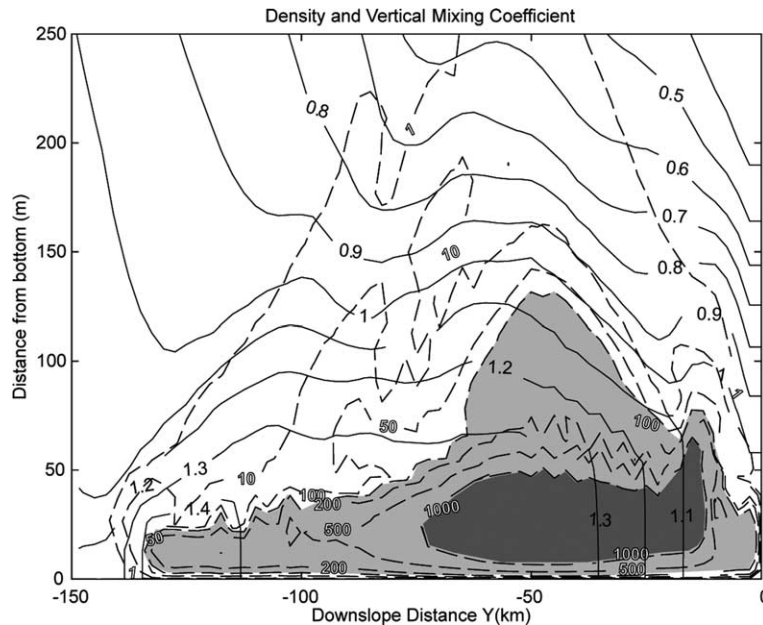


Fig. 3. Cross section at $x = -100$ km of density anomaly, $\Delta\sigma_T$, and vertical mixing coefficient, K_M , after a 40-days simulation with a sigma coordinates model with 2.5 km resolution, using the M–Y turbulence scheme. Density is relative to surface density and indicated by solid contours. Mixing coefficient is indicated by dashed contours; the light shaded area represents values between 10^2 and 10^3 $\text{cm}^2 \text{s}^{-1}$, the dark shaded area represents values above 10^3 $\text{cm}^2 \text{s}^{-1}$.

3.2. The effect of the turbulence scheme on diapycnal mixing and plume transport

There are two ways in which the turbulence scheme affects the plume dynamics, first through the diapycnal mixing associated with the vertical mixing coefficient for tracers, K_H , and second, through the effect that the mixing coefficient for momentum, K_M , has on the BBL dynamics and the BBL Ekman transport in particular (e.g., Fig. 3). To isolate those effects, two additional experiments are conducted with the 10 km sigma grid, one with $K_H = 0$ and one with $K_M = 0$; in Figs. 4 and 5 they are compared after 40 days with the control case using the Mellor–Yamada scheme. These three experiments will be referred to as KH0, KM0 and M–Y, respectively. Note that even without any external background vertical mixing (only small numerical diffusion may still exist), the model remains numerically stable. While the KH0 and KM0 experiments are extreme cases that only intend for model sensitivity purposes, they may for example represent special conditions with either a very heavy plume that does not mix much with the overlaying fluid (the KH0 case), or a frictionless plume on a very smooth bottom (the KM0 case).

In the control run (M–Y case, Figs. 4a and 5a) most of the plume dilution occurs at the first 100 km from the source. Therefore, relatively homogeneous plume is found farther downstream where horizontal diffusion and eddy mixing may also play a role. Without diapycnal mixing (KH0 case, Fig. 4b) the downslope side of the plume front remains relatively undiluted and thus extends further down until it reaches a depth with overlying waters of the same density. For example, bottom water with tracer concentration of 0.8 reaches 600 km downstream and 200 km downslope

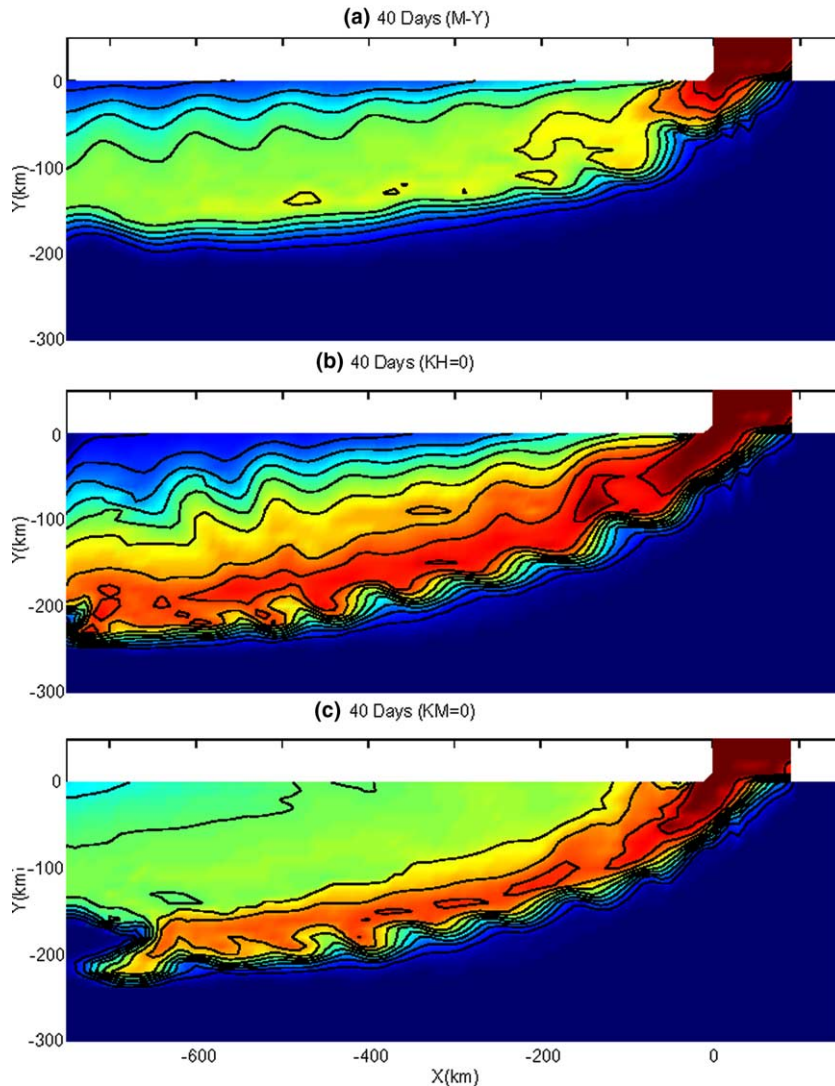


Fig. 4. Tracer concentration at the bottom layer after 40 days simulations with POMgcs using a sigma grid with 10 km resolution: (a) vertical mixing coefficients for tracers (K_H) and momentum (K_M) obtained from the Mellor–Yamada turbulence scheme (M–Y case); (b) setting $K_H = 0$ (KH0 case); (c) setting $K_M = 0$ (KM0 case).

from the source in this case, but only 50 km from the source in the M–Y case. The lack of diapycnal mixing results in a very thin BBL (Fig. 5b). In the KM0 case (Fig. 4c) the undiluted downslope side of the front is similar to the KH0 case (K_H is also reduced when K_M is eliminated), but the plume did not separate from the coast. A cross section of this case (Fig. 5c) reveals that a thick and vertically mixed part of the plume remains near the wall. Vertical profiles of tracer concentration, density and downslope velocity (Fig. 6) show that the diapycnal mixing in the M–Y case results in a thicker bottom mixed layer and a transition layer above the BBL, similar to the

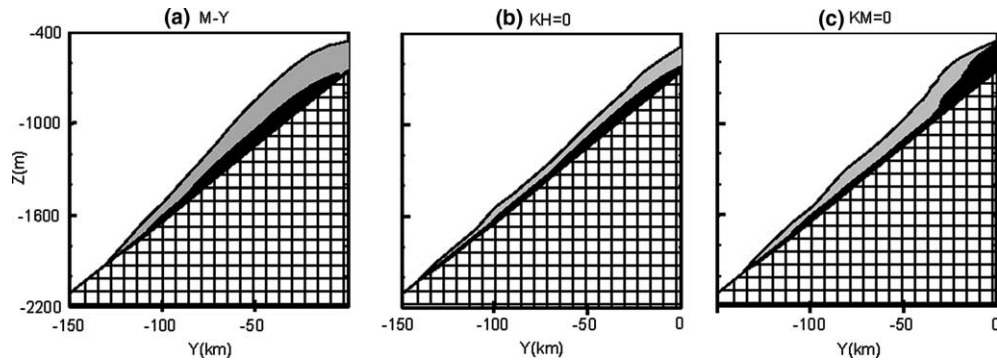


Fig. 5. Cross-section of tracer concentration, c , at $x = -100$ km after 40 days: (a) M–Y case (b) KH0 case; (c) KM0 case. The light shaded area represents $0.1 < c < 0.5$ and the dark shaded area represents $0.5 < c < 1$.

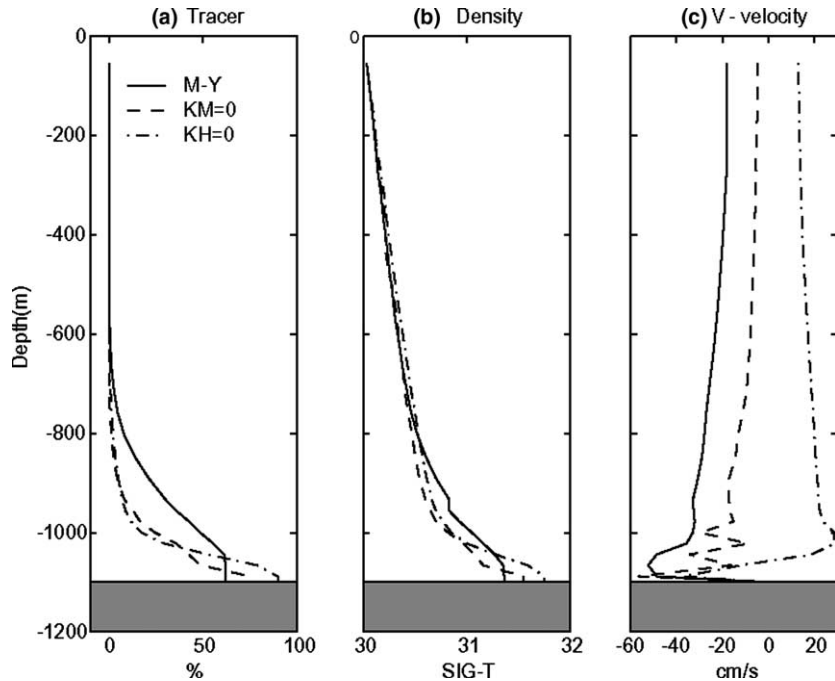


Fig. 6. Vertical profiles after 40 days at $(x, y) = (-100, -40)$ km. (a) Tracer concentration (% of maximum concentration of the source), (b) density (in σ_T units), (c) across slope velocity (v -component, in cm s^{-1}). Solid lines are for the M–Y case, dash lines are for the KM0 case and dash-dot lines are for the KH0 case.

observed profiles of Girton and Sanford (2003). In the KM0 case a negative velocity (downslope) is limited to a thin BBL of ~ 20 m from the bottom (Fig. 6c), while in the M–Y case a thicker BBL of about 75 m has a downslope velocity as large as 0.5 m s^{-1} .

The along-isobaths translation speed of dense frictionless eddies on a sloping bottom can be estimated by

$$u_t = g \frac{\Delta\rho}{\rho_0} \frac{s}{f} \quad (2)$$

(Nof, 1983), where s is the bottom slope, f the Coriolis parameter, g the gravitational acceleration, and $\Delta\rho/\rho_0$ the eddy's density anomaly relative to the background density. Recent laboratory experiments show that the along-isobaths velocity component of dense overflow plumes obeys a similar relationship (Cenedese et al., 2004). The same seems to be true for the model results. For example, in case KM0 (Fig. 4c) there seem to be two different downstream velocities, a faster one for the shallow side of the plume (at ~ 800 m) and a slower one in the deep part of the plume (at ~ 2500 m). Here $s = 0.01$, $f = 10^{-4} \text{ s}^{-1}$, and $g' = g\Delta\rho/\rho_0$ is $\sim 5 \times 10^{-3}$ and $\sim 2 \times 10^{-3} \text{ m s}^{-2}$ for the shallow and deep regions, respectively. Thus u_t is 0.5 m s^{-1} for the shallow region and 0.2 m s^{-1} for the deep region, very similar to the model bottom velocities in these regions, 0.4 and 0.23 m s^{-1} , respectively. While the along-isobaths plume flow seems to be simply proportional to the density anomaly (thus to diapycnal mixing upstream), the downslope velocity component of the plume is affected by pressure gradients, bottom friction and BBL dynamics. In particular, in the KM0 case the downslope Ekman transport (i.e., with component to the left of the along-isobaths flow) is reduced so that the along-isobaths component is much larger than the downslope component in the upper slope part of the plume.

It is possible now to estimate the contribution of the M–Y scheme to the downslope bottom Ekman transport. At $y = -100$ km the total downslope transport of the plume in the M–Y case is 9 Sv compared to 7 Sv for the KM0 case and compared to 5 Sv imposed outflow in the embayment. Therefore, about 2 Sv , or 22% of the transport, is contributed by the Ekman transport associated with the model mixing coefficient K_M .

Another important parameter that affects the propagation and stability of bottom plumes is the Froude number,

$$Fr = \frac{U_0}{\sqrt{g \frac{\Delta\rho}{\rho_0} h_0}} \quad (3)$$

where U_0 is the velocity scale, and h_0 the plume thickness scale. The imposed inflow is set such that the flow is just below the critical value ($Fr \leq 1$) in the embayment. Farther downstream, the values found in the model are mostly $0.4 < Fr < 0.6$, thus the flow is subcritical and resembling in the Fr values and in its structure the “eddy” regime found in the laboratory overflow experiments of Cenedese et al. (2004). Because of the existence of propagating eddies the simulated overflow does not reach steady state even after 40 days; observations of overflows also indicate considerable variability and eddy activities (Girton and Sanford, 2003). Therefore, additional mixing involves the action of eddies and other space and time-dependent variations in the flow. This can be seen by the vertically integrated vorticity balance equation,

$$\begin{aligned} \frac{\partial}{\partial t} \left(\frac{\partial VD}{\partial x} - \frac{\partial UD}{\partial y} \right) + \left(\frac{\partial A_y}{\partial x} - \frac{\partial A_x}{\partial y} \right) + \left(\frac{\partial(fUD)}{\partial x} + \frac{\partial(fVD)}{\partial y} \right) + \left(-\frac{\partial P_b}{\partial x} \frac{\partial D}{\partial y} + \frac{\partial P_b}{\partial y} \frac{\partial D}{\partial x} \right) \\ + \left(-\frac{\partial \tau_{yb}}{\partial x} + \frac{\partial \tau_{xb}}{\partial y} \right) = 0 \end{aligned} \quad (4)$$

where (U, V) are the vertically averaged velocity components, $D = H + \eta$ is the water depth plus surface elevation, (A_x, A_y) are the advection and diffusion terms, P_b is the bottom pressure, and (τ_x, τ_y) are the bottom stress components. The five terms in (4), the tendency term, the advection and diffusion term, the Coriolis term, the bottom pressure torque term, and the bottom stress term are calculated from the model results after 40 days and shown in Fig. 7 for a section 200 km downstream of the source. In the M–Y case eddies play a major role ~ 50 km offshore, as indicated by the large tendency term which is balanced by advection and bottom pressure (Fig. 7a). In the KH0 case (Fig. 7b) the active part of the plume is farther downslope ($y = -150$ km) where bottom stress and bottom pressure balance the tendency term. In this case the dynamics is dominated by the pressure gradients in the dense plume. In the KM0 case (Fig. 7c) there are two different regimes, one near the coast with similar vorticity balance as in the M–Y case, and one farther

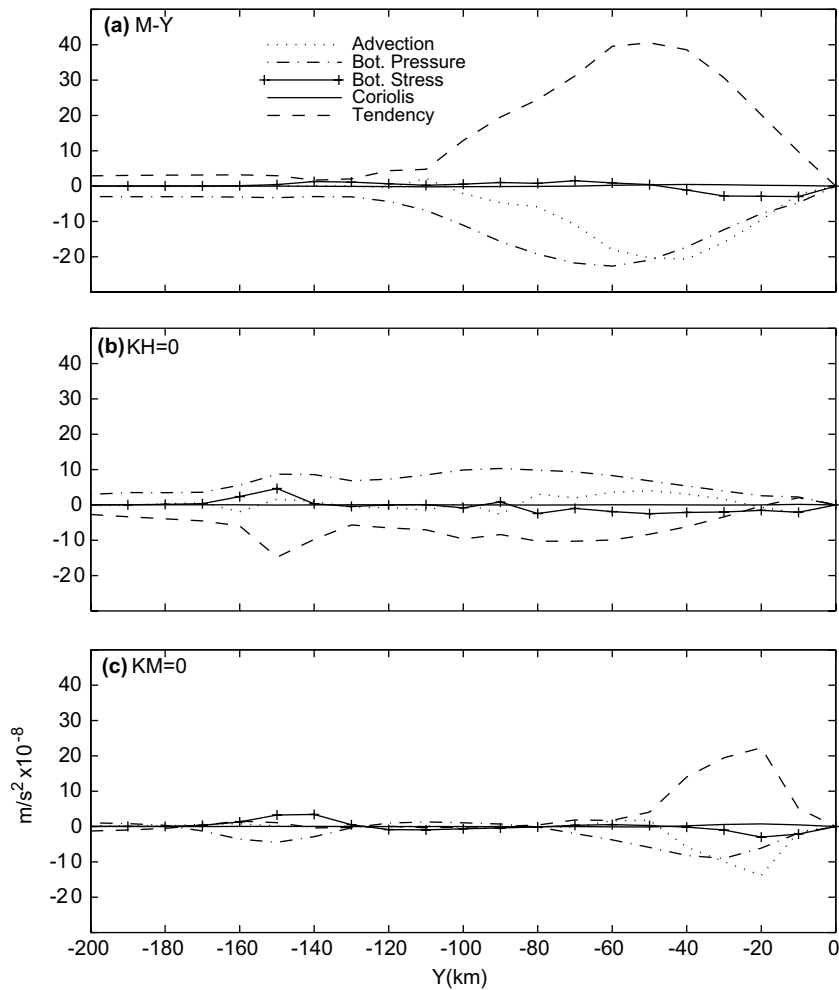


Fig. 7. The vertically integrated vorticity balance equation terms after 40 days at $x = -200$ km; (a) M–Y case, (b) KH0 case, and (c) KM0 case. The terms are advection and diffusion (dotted line), bottom pressure torque (dash-dot line), bottom stress (“+” line), Coriolis (solid line) and tendency (dashed line).

downstream at the edge of the plume where bottom stress and bottom pressure are the dominant terms. There are no significant vorticity terms between 60 and 130 km downslope, where homogeneous fluid is propagating in a constant speed along the isobaths (Fig. 4c).

To evaluate the diapycnal mixing with and without the M–Y scheme, a histogram of the tracer distribution as a function of downstream distance and density is used (Fig. 8); this diagram has been proposed by Hallberg (personal communication) and is also used in Legg et al. (in press) to evaluate z -level and isopycnal models. In the M–Y case (Fig. 8a) most of the diapycnal mixing occurs up to ~ 150 km from the source (located at the bottom-right corner of the diagram) and then the diluted plume settled at a density level with neutral buoyancy. Note that large part of the high density region ($\Delta\sigma_T > 1.4$, blue color) remain totally clear from any source waters. Fig. 8a closely resembles the histogram for the nonhydrostatic model of Legg et al. (in press). In the KH0 case (Fig. 8b) the larger concentration of source waters are found further downstream and in denser layers, there is no abrupt mixing near the source, and only very deep regions ($\Delta\sigma_T > 1.8$)

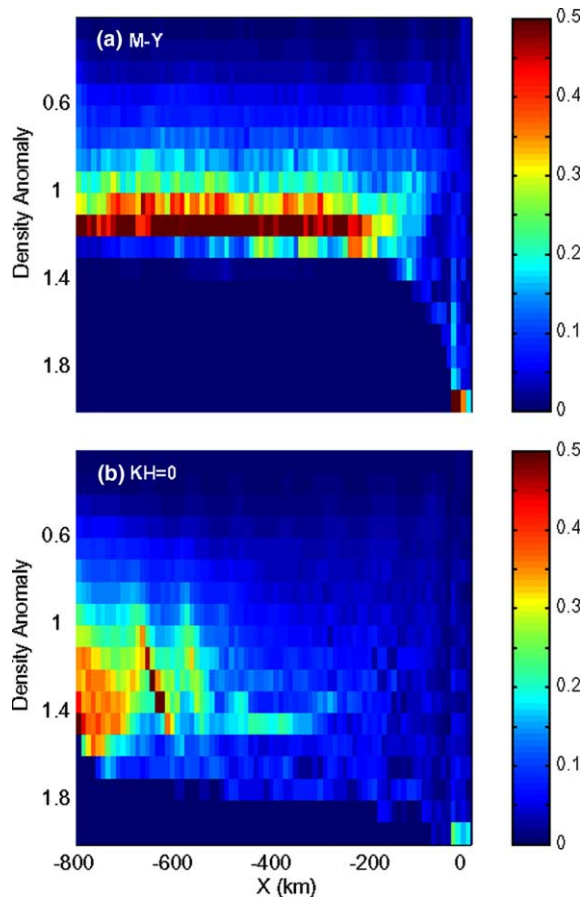


Fig. 8. Histogram of tracer concentration after 40 days as a function of downstream distance (x -axis) and density anomaly (y -axis). Density anomaly is in σ_T units relative to initial surface density (value of 0), whereas initial source water has a value of 2 (lower right corner of the histogram); (a) M–Y case and (b) KH0 case.

remain without any trace of source waters. Fig. 8b resembles results of the Hallberg Isopycnal Model (HIM) used in Legg et al. (in press).

As the plume propagating away from the source and entrained with overlaying waters, its volume and transport may change. This can be described by a simple mass balance equation,

$$\frac{\partial}{\partial x} \int_A U dA = \oint_L W_E, \quad (5)$$

where the left-hand side is the change in transport across a section A and the right-hand side is the total entrainment, integrating the entrainment velocity along the plume's edge. Defining the plume in the model by tracer concentration values greater than 0.01, the plume's downstream transport for the M–Y and for the KH0 cases after 40 days are shown in Fig. 9. In the M–Y case the transport increases from the imposed 5 Sv at the embayment to about 15 Sv at $x = -100$ km, indicating a strong diapycnal mixing (i.e., Fig. 8) and thus large entrainment (i.e., Eq. (5)) that increases the plume's volume. Further downstream the transport generally decreases (i.e., detrainment occurs). However, the oscillatory transport variation with a wavelength of ~ 100 km indicate small entrainment/detrainment associated with meandering and eddies. Observations may also indicate the possibility of some reduced transport, and thus some detrainment, for distances over 200 km from the source (Fig. 11 in Girton and Sanford, 2003). In the KH0 case on the other hand, the transport continues to increase, possibly indefinitely, but at least all the way to the western boundary at $x = -800$ km.

To summarize the distribution of the water mass that originated from the dense water overflow source, the zonally averaged (over the model east–west domain length, X) and vertically integrated tracer concentration is calculated by

$$C(y) = \frac{1}{X} \int_x \int_z c(x, y, z) dx dz, \quad (6)$$

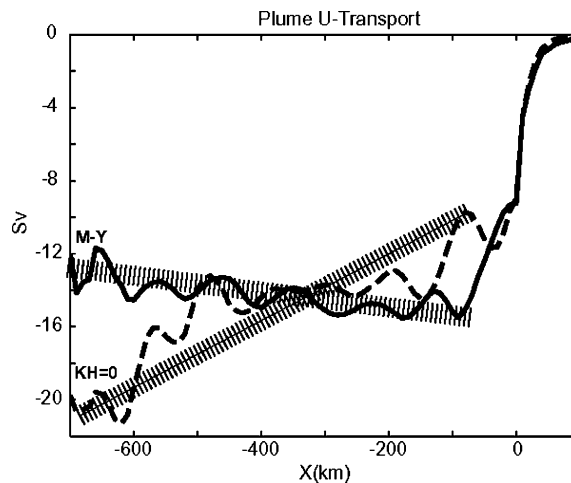


Fig. 9. Downstream plume transport as a function of x for the control run (M–Y case, solid line) and for the KH0 case (dashed line). The average slopes of the lines after the initial mixing (for $-700 \text{ km} < x < -100 \text{ km}$) are indicated; they show a decrease in plume transport (i.e., detrainment) for the M–Y case, but an increase in transport (i.e., entrainment) for the KH0 case.

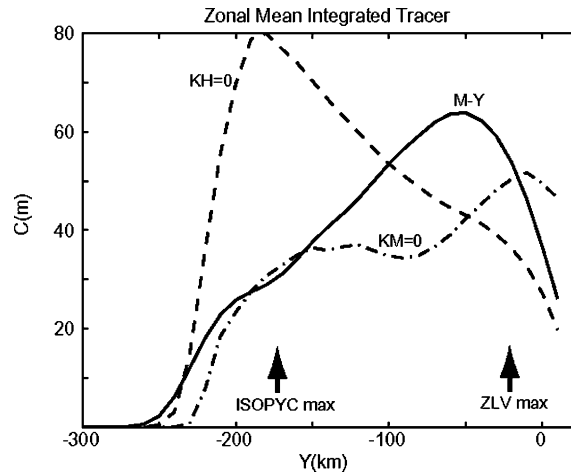


Fig. 10. Zonal mean and vertically integrated tracer, C , as a function of downslope distance. Solid line is for the M–Y case, dash line is for the KH0 case and dash-dot line is for the KM0 case. Also indicated by arrows are the locations of the maxima for the POMgcs z -level case of Fig. 2e (“ZLV max”) which is similar to the KM0 case and for results from the Hallberg Isopycnal Model, HIM (“ISOPYC max”) which is similar to the KH0 case.

and shown for day 40 in Fig. 10. C has units of meter and is proportional to the average thickness of the plume in the water column. In the M–Y control case the average plume thickness increases rapidly in the first 50 km and then gradually decreases until about 250 km downslope (see also Fig. 5a). The shape of the integrated tracer is opposite in the KH0 case, with gradual increase until almost 200 km downslope and then an abrupt decrease, the latter is the result of the sharp front seen in Fig. 4b. In the KM0 case, the amount of tracer has its maximum near the northern wall (see also Fig. 5c) and gradually decreases downslope. The difference between the M–Y and the KM0 cases (most visible between $y = -25$ and $y = -150$ km) represents the contribution of the BBL Ekman velocity to the downslope transport of source waters; the difference is maximum at about 100 km downslope where the Ekman transport accounts for $\sim 30\%$ of the total accumulated tracer. It is interesting to note that the tracer distribution in the KM0 case is somewhat similar to that of the z -level model of Fig. 4e (the location of the maximum in the z -level calculation is marked in Fig. 10 by “ZLV max”; the full structure is shown in Ezer and Mellor, 2004). This result supports the notion that the downslope Ekman transport is not well represented in z -level models with stepped topography (without special BBL schemes), as indicated by other studies (Winton et al., 1998; Pacanowski and Gnanadesikan, 1998; Ezer and Mellor, 2004). On the other hand, the tracer distribution in the case with no diapycnal mixing (KH0) is almost identical in its shape to DOME experiments done with an isopycnal model (HIM, the maximum of which is marked in Fig. 10 by “ISOPYC max”).

4. Discussion and conclusions

Recent studies of dense gravity currents associated with overflows from observations (Girton and Sanford, 2003) models (Jungclauss et al., 2001; Ozgokmen and Chassignet, 2002; Papadakis

et al., 2002; Käse et al., 2003; Ezer and Mellor, 2004; Legg et al., in press) and laboratory experiments (Cenedese et al., 2004), all indicate the complicated nature of the flow and the need to better understand the mixing processes involved. To improve simulations of overflows and deep ocean formation in climate models there is a need for better parameterization of diapycnal mixing and bottom boundary layers (Griffies et al., 2000). This study is a follow-up on the model intercomparison study of Ezer and Mellor (2004), who compared overflow simulations in terrain-following and in z -level grids using the generalized coordinate ocean model of Mellor et al. (2002). The focus of this study is on the role played by the Mellor–Yamada (M–Y) turbulence scheme when used in terrain-following ocean models, in determining the diapycnal mixing and the gravity current transport properties. An idealized overflow configuration (Dynamics of Overflow Mixing and Entrainment setting, DOME), is used by different groups (Ezer and Mellor, 2004; Legg et al., in press) to allow comparisons of different models and test different parameter-space regimes.

The dense plume in the DOME configuration is set with inflow velocity and plume thickness such that the Froude number is subcritical ($Fr \leq 1$), and thus in an eddy regime as in laboratory experiments (Cenedese et al., 2004) and in the Denmark Straits overflow (Jungclaus et al., 2001). This makes the representation of the overflow in coarse resolution models more difficult. Therefore, overflow simulations with z -level and terrain-following grids at 10 and 2.5 km resolutions are compared with results from a nonhydrostatic model with 0.5 km resolution (Legg et al., in press). The nonhydrostatic model provides some “model truth” for this idealized case (though the resolution is still marginal for full nonhydrostatic dynamics). The comparisons indicate too strong diapycnal mixing and not enough downslope transport in a z -level grid, which is a well known problem (Winton et al., 1998; Ezer and Mellor, 2004), unless the stepped topography is replaced by partial cells or special BBL schemes are added. However, a new finding is the great similarity between the results of a hydrostatic model with a terrain-following grid and the results of a very high resolution nonhydrostatic model. While only at 2.5 km resolution the details of the eddies shape are well simulated, even at 10 km resolution the extent of the bottom plume, its transport and its dilution match extremely well the nonhydrostatic results. This indicates that the subgrid-scale parameterization of turbulent mixing, obtained here from the M–Y turbulence scheme, is doing a decent job in two aspects: 1. the space and time-dependent vertical mixing coefficient for tracers, K_H , represents quite accurately the diapycnal mixing and entrainment of the plume, and 2. the vertical mixing coefficient for momentum, K_M , represents quite accurately the downslope bottom Ekman transport contribution to the plume’s total transport. Special experiments with either $K_H = 0$ or $K_M = 0$ isolate the M–Y influence and reveal interesting results. With no diapycnal mixing the plume in the terrain-following model closely resembles results from isopycnal models where the dense plume is driven by pressure gradients and slides farther downstream, with increasing transport. On the other hand, the results of the terrain-following model with reduced Ekman transport resemble results of a z -level model with stepped topography, where large part of the dense plume remains upslope and only propagated along isobaths. Although a simple z -level model with enough vertical resolution and a reasonable mixing coefficient will produce horizontal bottom Ekman transport, the cross isobaths velocity component is not directly translated into a downslope transport of the dense water, but requires vertical mixing (or other convective adjustment or BBL formulation) which may dilute the plume and creates excess diapycnal mixing. The M–Y turbulence scheme when used with a terrain-following grid seems to provide a reasonable compromise between the two extreme cases of a z -level like

solution with too much diapycnal mixing and an isopycnic-like solution with too little diapycnal mixing.

Although the DOME configuration is highly idealized and primarily intends to test various models and parameterizations, some of the basic observed characteristics of the Denmark Strait plume in Girton and Sanford (2003) are simulated quite well with the terrain-following model. The maximum velocity in the bottom layer range from 0.2 to 1.4 m s^{-1} in the model and in the observations, the along-isobath velocity component in the model is proportional to the density anomaly and to the slope divided by the Coriolis parameter, similar to the translation of dense eddies on a sloping bottom (Nof, 1983), and as measured in laboratory experiments of overflows (Cenedese et al., 2004). The average plume thickness is about 240 m in the model and 40–400 m in the observations. In the model, the plume descends downslope by about 1000 m within 200 km from the source, only slightly less than the observed descent, with strong entrainment near the source that dilutes the plume and increases the plume transport. In the model, the transport tripled within the first 100 km from the source and then gradually decreases for the next 700 km downstream, indicating possible detrainment far from the source. Estimating the plume transport from cruise sections and current meter arrays shows large uncertainty (Fig. 11 in Girton and Sanford, 2003), but at 150 km from the source the observed transport seems to be 2–3 times the source transport, and there is some indication for reduced transport farther than 150 km from the source, as seen in the model. Combining the results of various idealized and realistic models with new observations of overflows will eventually lead to better parameterization of such flows in ocean models, and better understanding of their dynamics.

Acknowledgements

This study is part of the Climate Process Team-Gravity Current Entrainment (CPT-GCE) project, supported by NSF award # OCE-0336768. All the CPT team members are thanked for many useful discussions, and in particular Sonya Legg and Bob Hallberg who provided results from the MIT and HIM models prior to publication which were essential for the comparison with the terrain-following model. Additional support is provided by the Office of Naval Research (ONR), award # N00014-04-10381. Comments by George Mellor and two anonymous reviewers were helpful to improve the manuscript. Computational resources were provided by the High-Performance Computing System (HPCS) at NOAA's Geophysical Fluid Dynamics Laboratory (GFDL).

References

- Adcroft, A., Hill, C., Marshall, J., 1997. Representation of topography by shaved cells in a height coordinate ocean model. *Monthly Weather Review* 125, 2293–2315.
- Beckmann, A., Döscher, R., 1997. A method for improved representation of dense water spreading over topography in geopotential-coordinate models. *Journal of Physical Oceanography* 27, 581–591.
- Blumberg, A.F., Mellor, G.L., 1987. A description of a three-dimensional coastal ocean circulation model. In: Heaps, N.S. (Ed.), *Three-Dimensional Coastal Ocean Models*. In: *Coastal Estuarine Studies*, vol. 4. American Geophysical Union, Washington, DC, pp. 1–16.

- Campin, J.-M., Goosse, H., 1999. Parameterization of density-driven downsloping flow for a coarse-resolution ocean model in z-coordinate. *Tellus* 51A, 412–430.
- Cenedese, C., Whitehead, J.A., Ascarelli, T.A., Ohiwa, M., 2004. A dense current flowing down a sloping bottom in a rotating fluid. *Journal of Physical Oceanography* 34, 188–203.
- Ezer, T., 2000. On the seasonal mixed-layer simulated by a basin-scale ocean model and the Mellor–Yamada turbulence scheme. *Journal of Geophysical Research* 105, 16,843–16,855.
- Ezer, T., Arango, H., Shchepetkin, A.F., 2002. Developments in terrain-following ocean models: Intercomparisons of numerical aspects. *Ocean Modelling* 4, 249–267.
- Ezer, T., Mellor, G.L., 2004. A generalized coordinate ocean model and a comparison of the bottom boundary layer dynamics in terrain-following and in z-level grids. *Ocean Modelling* 6, 379–403.
- Ezer, T., Weatherly, G.L., 1990. A numerical study of the interaction between a deep cold jet and the bottom boundary layer of the ocean. *Journal of Physical Oceanography* 20, 801–816.
- Gerdes, R., 1993. A primitive equation ocean circulation model using a general vertical coordinate transformation. 1. Description and testing of the model. *Journal of Geophysical Research* 98, 14,683–14,701.
- Girton, J.B., Sanford, T.B., 2003. Descent and modification of the overflow plume in the Denmark Strait. *Journal of Physical Oceanography* 33, 1351–1364.
- Griffies, S.M., Boning, C., Bryan, F.O., Chassignet, E.P., Gerdes, R., Hasumi, H., Hirst, A., Treguier, A., Webb, D., 2000. Developments in ocean climate modelling. *Ocean Modelling* 2, 123–192.
- Haidvogel, D.B., Arango, H., Hedstrom, K., Beckmann, A., Malanotte-Rizzoli, P., Shchepetkin, A.F., 2000. Model evaluation experiments in the North Atlantic basin: Simulations in nonlinear terrain-following coordinates. *Dynamics of Atmospheres and Oceans* 32, 239–282.
- Hallberg, R.W., 2000. Time integration of diapycnal diffusion and Richardson number dependent mixing in isopycnal coordinate ocean models. *Monthly Weather Review* 128, 1402–1419.
- Jiang, L., Garwood Jr., R.W., 1996. Three-dimensional simulations of overflows on continental slopes. *Journal of Physical Oceanography* 26, 1214–1233.
- Jungclauss, J.H., Mellor, G.L., 2000. A three-dimensional model study of the Mediterranean outflow. *Journal of Marine Systems* 24, 41–66.
- Jungclauss, J.H., Hauser, J., Käse, R.H., 2001. Cyclogenesis in the Denmark Strait overflow plume. *Journal of Physical Oceanography* 31, 3214–3229.
- Käse, R.H., Girton, J.B., Sanford, T.B., 2003. Structure and variability of the Denmark Strait overflow: Model and observations. *Journal of Geophysical Research* 108 (C6), doi: [10.1029/2002JC001548](https://doi.org/10.1029/2002JC001548).
- Killworth, P.D., Edwards, N.R., 1999. A turbulent bottom boundary layer code for use in numerical models. *Journal of Physical Oceanography* 29, 1221–1238.
- Legg, S., Hallberg, R.W., Girton, J.B., in press. Comparison of entrainment in overflows simulated by z-coordinate, isopycnal and nonhydrostatic models. *Ocean Modelling*.
- Marshall, J., Jones, H., Hill, C., 1998. Efficient ocean modeling using nonhydrostatic algorithms. *Journal of Marine Systems* 18, 115–134.
- Martin, P.J., 1985. Simulation of the mixed layer at OWS November and papa with several models. *Journal of Geophysical Research* 90, 903–916.
- Mellor, G.L., Yamada, T., 1982. Development of a turbulent closure model for geophysical fluid problems. *Review of Geophysics* 20, 851–875.
- Mellor, G.L., Hakkinen, S., Ezer, T., Patchen, R., 2002. A generalization of a sigma coordinate ocean model and an intercomparison of model vertical grids. In: Pinardi, N., Woods, J.D. (Eds.), *Ocean Forecasting: Conceptual Basis and Applications*. Springer, pp. 55–72.
- Nof, D., 1983. The translation of isolated cold eddies on a sloping bottom. *Deep-Sea Research* 30, 171–182.
- Ozgoekmen, T.M., Chassignet, E., 2002. Dynamics of two-dimensional turbulent bottom gravity currents. *Journal of Physical Oceanography* 32, 1460–1478.
- Pacanowski, R.C., Gnanadesikan, A., 1998. Transient response in a z-level ocean model that resolves topography with partial cells. *Monthly Weather Review* 126, 3248–3270.
- Papadakis, M.P., Chassignet, E.P., Hallberg, R.W., 2002. Numerical simulations of the Mediterranean sea outflow: Impact of the entrainment parameterization in an isopycnal coordinate ocean model. *Ocean Modeling* 5, 325–356.

- Price, J.F., Barringer, M.O., 1994. Outflows and deep water production by marginal seas. *Progress in Oceanography* 33, 161–200.
- Song, Y.T., Chao, Y., 2000. An embedded bottom boundary layer formulation for z-coordinate ocean models. *Journal of Atmospheric and Oceanic Technology* 17, 546–560.
- Song, Y.T., Haidvogel, D., 1994. A semi-implicit ocean circulation model using a generalized topography following coordinate system. *Journal of Computational Physics* 115, 228–248.
- Warner, J.C., Sherwood, C.R., Arango, H.G., Signell, R.P., in press. Performance of four turbulence closure models implemented using a generic length scale method. *Ocean Modelling* 7.
- Winton, M., Hallberg, R.W., Gnanadesikan, A., 1998. Simulation of density-driven frictional downslope flow in z-coordinate ocean models. *Journal of Physical Oceanography* 28, 2163–2174.